

---

# **Experimental Verification of Cooling Load Calculations for Spaces with Non-Uniform Temperature Radiant Surfaces**

*ASHRAE 1729-TRP Project*

---

## **Prepared by**

Dr. Atila Novoselac – Principle Investigator

Dr. Stephen Bourne – Research Assistant

Ardeshir Moftakhari – Research Assistant

## **Contact Information**

Department of Civil, Environmental and Architectural Engineering

University of Texas at Austin

5.422 ECJ, 1 University Station C 1752

Austin, TX 78712-1076

512-905-4917

---

# CONTENTS

---

Experimental Apparatus .....	7
Experimental Facility.....	7
Measurement Instrumentations.....	8
Uncertainty Analysis.....	9
Experimental Program.....	11
Experimental Protocols.....	11
Experimental Matrix.....	11
Summary of Experimental Test.....	12
Experiment No. 1: Radiant panel vs All-Air system under solar and radiative loads.....	12
Experiment No. 2: Radiant panel vs All-Air system with internal loads.....	16
Experiment No. 3: Radiant panel vs All-Air system with constant internal loads.....	21
Experiment No. 4: Radiant panel vs All-Air system with internal loads in typical office working schedule .....	24
Experiment No. 5: Radiant panel vs All-Air system cooling performance under dominant solar load .....	27
References .....	30

---

## LIST OF FIGURES

---

<b>Fig.1:</b> Test chambers at Thermal Façade Laboratory.....	5
<b>Fig. 2:</b> Experimental setups, Radiant cooling sources configurations and temperature sensor map in Test chambers.....	7
<b>Fig. 3:</b> Solar, Radiative and Total Heat gains for the full-scale experiment during August 1 <sup>st</sup> to August 5 <sup>th</sup> .....	10
<b>Fig.4:</b> Net sensible space cooling rate for the full-scale experiment during August 1 <sup>st</sup> to August 5 <sup>th</sup> .....	11
<b>Fig.5:</b> Wall surface, mean radiant and air temperatures for the full-scale experiment during August 1 <sup>st</sup> to August 5 <sup>th</sup> .....	12
<b>Fig.6:</b> The configuration of internal radiative and convective heater sources for the full-scale experiment.....	14
<b>Fig.7:</b> Solar, internal convective, radiative heat gains for the full-scale experiment during August 9 <sup>th</sup> to August 14 <sup>th</sup> .....	15
<b>Fig.8:</b> Net space cooling rate for the full-scale experiment during August 9 <sup>th</sup> to August 14 <sup>th</sup> .....	16
<b>Fig.9:</b> Wall surface, air temperature profiles for the full-scale experiment during August 9 <sup>th</sup> to August 14 <sup>th</sup> .....	17
<b>Fig.10:</b> Solar, internal convective, radiative heat gains for full-scale experiment during August 17 <sup>th</sup> to August 20 <sup>th</sup> .....	19
<b>Fig.11:</b> Net space sensible cooling rate for full-scale experiment during August 17 <sup>th</sup> to August 20 <sup>th</sup> .....	19
<b>Fig.12:</b> Wall surface, MRT, Air temperatures for full-scale experiment during August 17 <sup>th</sup> to August 20 <sup>th</sup> .....	20
<b>Fig.13:</b> Solar, internal convective, radiative heat gains for full-scale experiment during August 22 <sup>nd</sup> to August 24 <sup>th</sup> .....	22
<b>Fig.14:</b> Net space sensible cooling rate for full-scale experiment during August 22 <sup>nd</sup> to August 24 <sup>th</sup> .....	22
<b>Fig.15:</b> Wall surface, MRT, Air temperatures for full-scale experiment during August 22 <sup>nd</sup> to August 24 <sup>th</sup> .....	23
<b>Fig.16:</b> Solar, internal convective, radiative heat gains for full-scale experiment during August 31 <sup>st</sup> to September 3 <sup>rd</sup> .....	25
<b>Fig.17:</b> Net space sensible cooling rate for full-scale experiment during August 31 <sup>st</sup> to September 3 <sup>rd</sup> .....	25
<b>Fig.18:</b> Wall surface, MRT, Air temperatures for full-scale experiment during August 31 <sup>st</sup> to September 3 <sup>rd</sup> .....	26

---

## LIST OF TABLES

---

<b>Table 1:</b> List of instrumentation used and measurement accuracy .....	7
<b>Table 2:</b> Experimental matrix of finished experiments .....	11

---

## **ACKNOWLEDGMENT**

---

The authors would like to express their sincere gratitude toward the dear committee members for their useful comments, suggestions, guidance, and criticism during the ASHRAE 1729-TRP project meetings.

---

# 1 EXPERIMENTAL APPARATUS

---

## 1-1: Experimental Facility

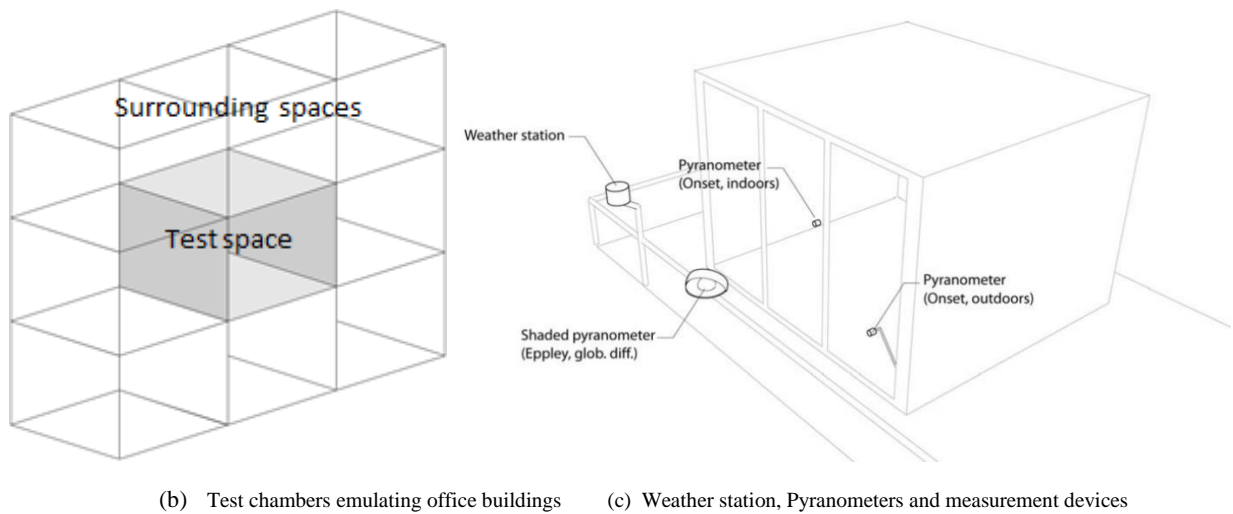
Two identical test chambers were used to perform a set of comparative experiments on cooling performance of radiant panel versus all-air system in the-state-of-Art Thermal Façade Laboratory at University of Texas in Austin, illustrated in Figure 1-a. The main purpose of the test chambers is to represent typical office spaces exposed to environmental conditions as well as internal occupancy patterns. The mid-sized test chambers are placed outdoors on a steel deck six meters above the street below. All external walls of the test chambers are exposed to outdoor weather conditions with a large façade on southern side of each chamber. As shown in Figure 1-b, the test chambers are employed to emulate cooling load, particularly in commercial buildings, where total heat exchange is almost negligible among adjacent office spaces. The state-of-art facility enables precise measurement of environmental heat gain, such as solar radiation, heat conduction, etc., entering the test chambers during daily operation as shown in Figure 1-c.

The structure of each test chamber is composed of a spacious glass façade on the south side, coupled with wall/ceiling/floor panels on the remaining sides that are heavily insulated to minimize thermal energy exchange with the outdoor environment. The glass façade is comprised of an outer pane of 0.006 (m) low-E glass, a 0.013 (m) argon-filled gap and a 0.006 (m) clear glass inner pane. The total size of the façade is 3.58 (m)×2.64 (m), which is divided into three separate windows by vertical dividers. The external walls and ceiling are comprised of similar materials; from interior to exterior: 0.032 (m) Gypsum drywall, 0.11 (m) Fiberglass-reinforced polyisocyanurate (FRP), 0.102 (m) structural insulated panel (SIP), 0.013 (m) Cementous panel over air gap with average U-value of 0.1067 (W/m<sup>2</sup>.K). This results in an average U-value of 0.085 (W/m<sup>2</sup>.K). The total net size of each test chamber is 3.62 (m)×3.98 (m)×2.82 (m). The floor is comprised of the following materials: 0.003 (m) gray carpet, 0.038 (m) plywood, 0.11 (m) fiberglass-reinforced polyisocyanurate, 0.102 (m) SIP and covered with 0.1 (m) of concrete blocks on its surface. The structure of each test chamber is well-sealed to prevent infiltration from the outdoor environment.

Each test chamber includes three parallel radiant cooling panel, that are installed at a height of 2.5 (m) in the ceiling. The size of each radiant panel is 2.4 (m) ×0.65 (m) per each, as it is shown in Figure 2-b. The Areo-Tech radiant cooling panels were composed of copper tubes mechanically bonded to an aluminum extrusion sheet. The copper tubes are connected to a hydronic piping loop. To minimize heat loss from the copper tubes, a 0.2 (m) cotton fiberglass insulation layer was utilized to fill the air gap on the top side of copper tubes to the ceiling. A dedicated chilled water system is responsible for supplying chilled water to the radiant panels. The dedicated chiller uses single-phase water - propylene glycol mixture as a working fluid. The total cooling capacity of the dedicated chilled water system was 2.0 (TONR), which can be modulated according to load by controlling supply water temperature, flow rate, or fan speed (cooling coil).



(a) Thermal façade lab in University of Texas at Austin



(b) Test chambers emulating office buildings      (c) Weather station, Pyranometers and measurement devices

**Figure 1:** Test chambers at Thermal Façade Laboratory

The use of radiant panels reduces the amount of heat accumulation in the thermal mass within the test chamber. 180 Concrete blocks (0.4 (m) × 0.19 (m) × 0.05 (m)) have been placed on the floor to mimic the effects of thermal mass found in actual office buildings. Altering the density and depth of concrete blocks modulates the effect of thermal mass in the test chambers. A portion of heat gain is absorbed into the concrete blocks, which is later released into the space to be removed by the cooling equipment.

## 1-2: Measurement Instrumentations

Table 1 outlines the equipment employed to precisely measure temperatures, heat fluxes, flow rates, etc. in the test chambers. To analyze heat transfer, a set of Omega 44033 thermistors were deployed to measure temperature on wall surfaces as shown in Figure 2-a. The Omega 44033 thermistors utilized to measure surface temperature have an accuracy of  $\pm 0.1$  C. These thermistors were placed around the test chamber as represented in Figure 2-c. There were 46 thermistors integrated into wall surfaces to measure surface temperatures. These were covered with tape to mimic thermal properties of the walls in the test chambers. There were 9 distinct thermistors positioned on the active cooled surface of the radiant cooling panels for temperature measurement. Additionally, a combination of 6 thermistors placed on the concrete blocks facilitated surface floor temperature measurements. Six thermistors were installed on a vertical stand at standard height levels (0.1, 0.6, 1.1, 1.6, 2.1, 2.6 m) to monitor both Mean Radiant Temperature (MRT) and ambient temperature, while specific thermistors were deployed to measure supply and return air

temperatures on supply and return vents. On the façade, a set of 9 thermistors were employed for window surface temperature measurement; these thermistors were covered with metallic tape to prevent solar radiative heat gain from the space or external sources. In Figure 2-d, the general arrangement of temperature sensors is presented in further detail.

A Davis Vantage Pro-Plus Weather Station was installed outside the test chambers to monitor environmental conditions. This device is capable of measuring air temperature with accuracy of  $\pm 0.5$  C, wind velocity and direction with accuracy of  $\pm 5\%$  using Davis Anemometer 6410, and global solar radiation with a silicon photodiode type pyranometer with an accuracy of  $\pm 5\%$  with  $\pm 2\%$  drift per year. An Eppley Precision Spectral Pyranometer (PSP) with an accuracy of  $\pm 1\%$  was used in calculating WWR, which was field-calibrated. Additionally, an onset silicon pyranometer (S-LIB-M003) was installed in the southern side of the test chambers outdoors to monitor global horizontal radiation. The Davis Vantage pyranometer was calibrated during a three-day-reading period using a linear correlation function ( $R^2 = 0.973$ ). Another Eppley PSP was utilized for measuring global diffused solar radiation flux transmitted into the chamber; this PSP was located at mid-window on a metal strand in the test chamber.

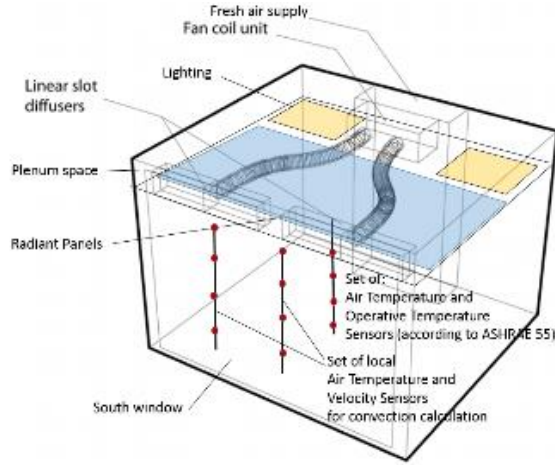
A set of temperature sensors were deployed on the hydronic loop to monitor chilled water properties during the operation of radiant cooling panels. The Omega 44033 thermistors were used to measure water temperature on the copper inlet and outlet pipes of the cooling coil with an accuracy of  $\pm 0.1$  C. To insure the accuracy of temperature differences, thermistors used in this application were field-calibrated as a pair. An Omega FTB-4605 flow meter was used to determine chilled water flow rate in the radiant cooling loop with an accuracy of  $\pm 2\%$ . These are field-calibrated using a linear correlation function ( $R^2 = 0.9995$ ) between flow rate and output signal meter. A single-phase water-propylene glycol mixture (35% propylene glycol) was used as a working fluid, with constant density and specific heat capacity assumed within the operating temperature range of the experiments.

### 1-3: Uncertainty Analysis

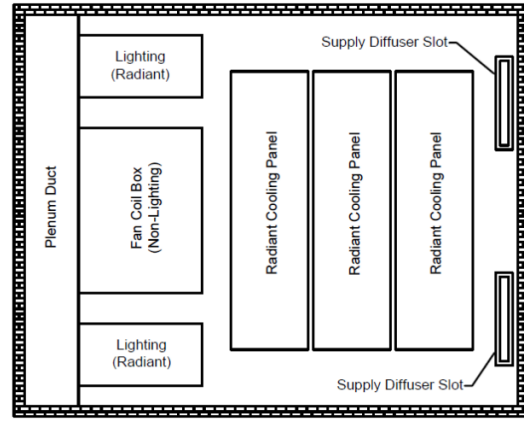
Uncertainty analysis is generally employed to analyze the measurement precision of experiments. The concept of uncertainty is basically the imprecision inherent in all measured variables for calculation of a reported value in the experiment. Common uncertainty analysis guidelines are ISO, JCGM, etc. implemented for precise data analysis in field measurements and calculation. Total heat flux from radiant cooling panels is a function of numerous measured variables including those associated with simultaneous effects of convection, radiation and conduction in the test chamber. The aforementioned variables contain surface area, air flow rate, surface temperature, solar radiation flux, supply and return air temperatures, conductivity coefficient, emissivity, etc., respectively. The general form of uncertainty analysis can be presented with the following equation:

$$\varphi = f(u_1, u_2, u_3, \dots, u_n) \quad (1)$$

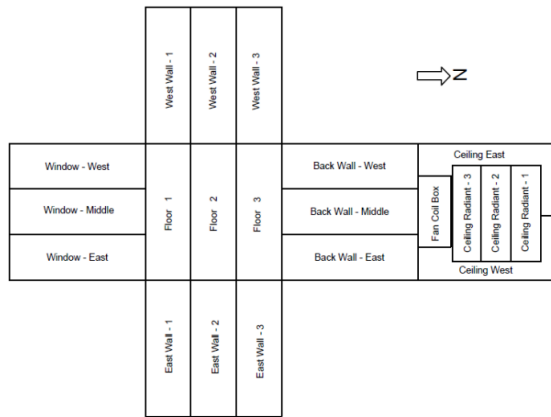
where  $\varphi$  and  $u_i$  are objective measured function and dependent variables. In this study, we employed the general theory of uncertainty analysis introduced by ASHRAE 2000 as follows:



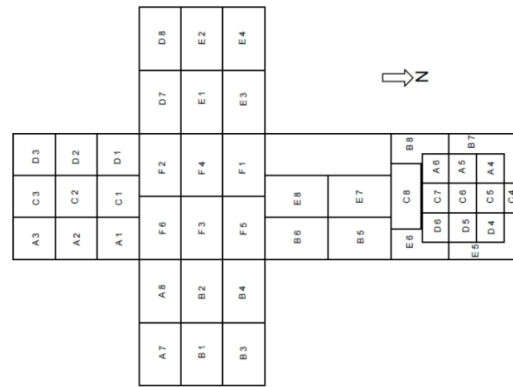
(a) Experimental setups, equipment and air temperature sensors



(b) Radiant source configurations and their locations



(c) Surface map in the test chambers



(d) Default Temperature sensor map positions in Test chambers

**Figure 2:** Experimental setups, Radiant cooling sources configurations and temperature sensor map in Test chambers

**Table 1:** List of instrumentations with their measurement accuracy

Variables	Instrument used	Measurement Accuracy
Surface Temperature	Omega 44033 thermistors	$\pm 0.1$ (c)
Coil Water temperature	Omega 44033 thermistors	$\pm 0.1$ (c)
Coil flow rate	Omega FTB-4506	2% of measured value
Specific heat and density of fluid	Experimentally tested	Assumed constant over operating range
Internal equipment loads	Brand Electronic ONE power meter Watt's up power meter	$\pm 1$ %
Global horiz. Radiation	Eppley Pyranometer	Within $\pm 1\%$ of WRR
Transmitted radiation (interior)	Apply PSP	Within $\pm 1\%$ of WRR
Outdoor air temperature	Davis External temp sensor	$\pm 0.5$ (c) under 43 (c)
Wind direction	Davis Anemometer 6410	$\pm 4$ degrees
Wind speed	Davis Anemometer 6410	Greater of $\pm 3$ (km/h) or $\pm 5\%$
Precipitation	Davis Rain collector II	Calibrated 0.01" (0.003 m) increments

$$\delta\varphi = \sqrt{(\delta u_1 \frac{\delta\varphi}{\delta u_1})^2 + (\delta u_2 \frac{\delta\varphi}{\delta u_2})^2 + \dots + (\delta u_n \frac{\delta\varphi}{\delta u_n})^2} \quad (2)$$

where  $n$  is total number of parameters,  $\delta u$  is uncertainty of certain parameter,  $\delta\varphi$  uncertainty in objective value,  $\frac{\delta\varphi}{\delta u_n}$  is changes in objective value with a unit change of the parameter.

---

## 2 EXPERIMENTAL PROGRAMME

---

### 2-1: Experimental Protocols

A fan coil cooling system with variable supply air temperature was used to represent an all-air system. The Air Exchange Rate per Hour (ACH) was modulated by controlling fan speed. This system was capable of maintaining a maximum cooling capacity of 1800 (W) per chamber while maintaining ventilation requirements for office spaces according to ASHRAE 62.1. Radiant cooling panels, capable of extracting maximum heat load of 850 (W) under realistic scenarios, were combined with an air ventilation system to represent a chilled ceiling panel cooling system. Both the radiant panel and all-air systems underwent a one-day preconditioning cycle to capture incremental changes in load before running full-scale experiments in both test chambers. The duration of each experiment was individually determined so as to be sufficiently long to capture typical cyclic cooling load changes resulted from environmental parameters, internal loads, etc. The duration of experiments varied from hours to days for different load scenarios.

### 2-2: Experimental Matrix

The experimental matrix is shown in Table 2. Each experiment is represented by a short description for specific test scenarios. The overall purpose of the studies listed in Table 2 was to examine the cooling performance of radiant panels compared with an all-air system, and to quantify the effects of different load scenarios, such as solar, pure convective load, dominant radiative loads, etc. A primary goal is to determine differences in the heat transfer dynamics of radiant panels verse an all-air system in the test chambers.

Table 2 Experimental matrix of finished experiments

No. of Case Study	Studied Phenomena Description	Case Condition Description
1	Effect of solar and radiative heat gains	Cooling performance of Radiant panel with no air vs. All-Air system under constant radiative heat gain by side radiative resistive panels and daily solar heat gain
2	Effect of internal convective and radiative loads	Cooling performance of Radiant panel with air vs. All-Air system under internal convective and radiative heat gains provided by side panel and internal cylinder and box heaters
3	Effect of constant internal loads	Cooling performance of Radiant panel with air vs. All-Air system under solar and constant internal heat gains provided by interior cylinder and box heaters
4	Effect of ON-OFF typical office working schedule	Cooling performance of Radiant panel with air vs. All-Air system under solar and internal heat gains according to ON-OFF working schedule in typical office spaces
5	Effect of Dominant Solar heat gain	Cooling performance of Radiant panel with air vs. All-Air system under dominant solar heat gain with ON-OFF working schedule for the cooling system in typical office spaces

---

## 3 EXPERIMENTAL MEASUREMENT TESTS

---

### 3-1: Experiment No. 1: Radiant panel vs All-Air system under solar and radiative loads

The main purpose of the first full-scale experiment was to evaluate the cooling performance of radiant panel versus all-air systems under dominant solar load. In order to do this, we set both test chambers to operate under purely radiative heat gain continuously for five days from August 1<sup>st</sup> to August 5<sup>th</sup>. The solar radiation was entering from the south-facing façade into each test chamber and was continuously measured with Eppley PSP throughout the experiment. The incident solar radiation causes temperature increase of interior walls, whose surface temperatures were measured by Omega 44033 thermistors and recorded by GW Instruments i100 data acquisition hardware. The test chambers were subject to daily solar radiation along with radiative heat gain by resistive side panel, constantly providing 300 (W, into the conditioned space. From weather data records, it was noted that the weather was partly cloudy but mostly sunny during the five-day experiment at Austin, TX.

The present experiment primarily investigates a comparison between radiant panel and all-air system for space cooling in both test chambers. In the first test chamber, radiant cooling panel was responsible for space cooling under dominant radiative load. The radiant cooling panel was capable of maintaining constant zone air temperature in the room using a controller developed using National Instruments hardware and LabView programming environment. The temperature sensor used for control purposes was installed in the return air vent. The radiant panel controller modulates a valve that supplies chilled water into the radiant panel loop in order to maintain a specified zone air set point temperature. During daily operation, radiant cooling panel removes space heat generated by both solar heat gain and radiative side panels installed on the west wall of the labs to mimic heat gain in a typical office building. The radiative side panel was operating from 8:00 AM to 6:00 PM every day, which represents internal load in typical office buildings. In the second test chamber, an all-air system was responsible to provide cooling. The second test chamber was similarly subjected to solar and side panel radiative heat gains. The solar radiation heat gain is presented for five-day operation of both test chambers in Figure 3, which also shows the operating schedule of the radiative side panels. Additionally, total heat gain can be calculated as the summation of solar radiation, radiative heat gain by side panel and electric load, as shown in Figure 3. The all-air system removes a major portion of heat by convection, while the radiant panel extracts space heat directly by radiation and indirectly by cooling surrounding wall surfaces. It is important to note that the radiant cooling panels directly remove a major portion of solar radiation and radiative heat gain generated by side panels.

From a cooling point of view, the cooling performance of radiant panel and all-air system can be evaluated through a comparison of the results for this five-day experiment. The amount of sensible heat removed by radiant panels from the first room should be equal to the heat

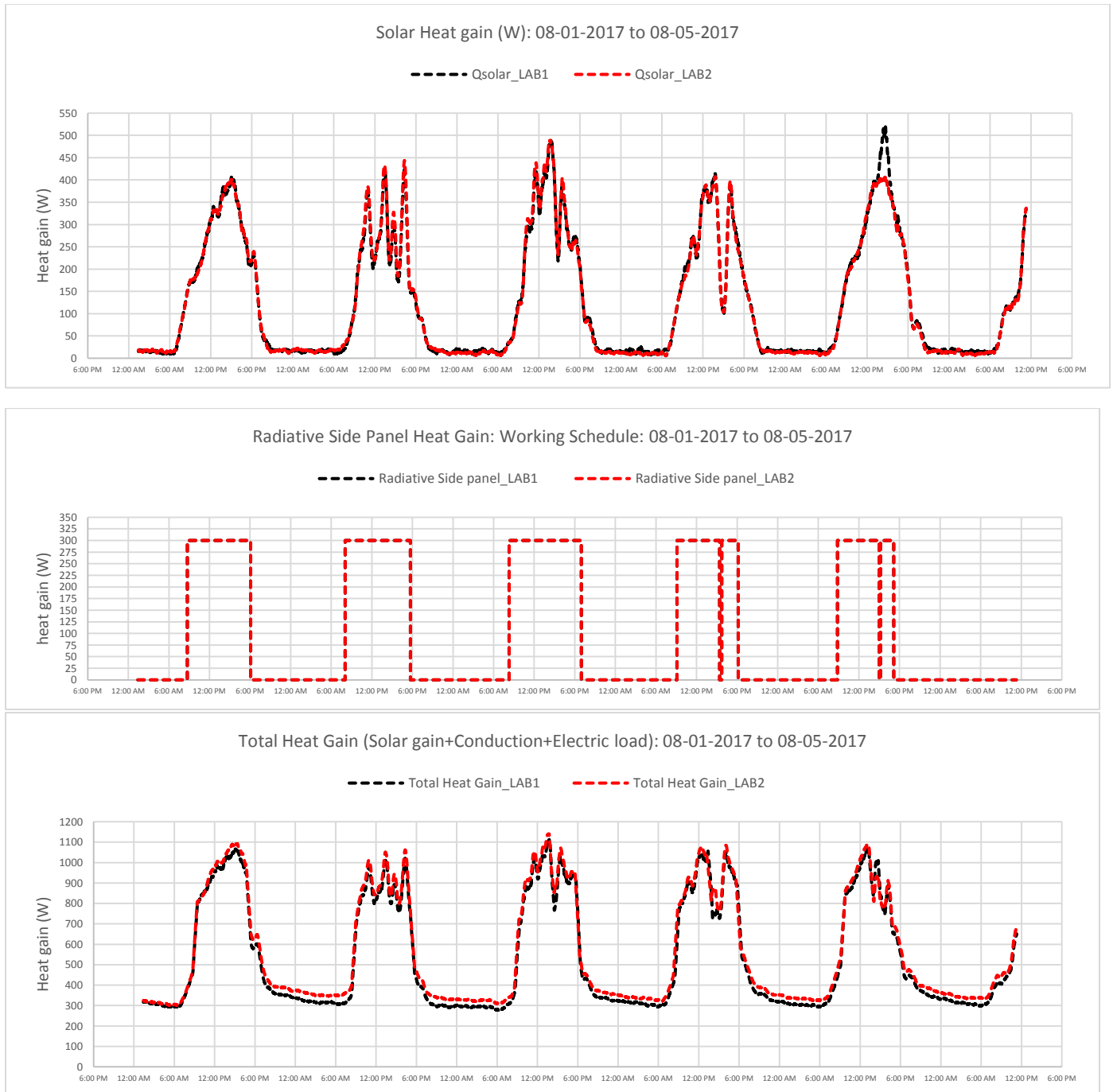


**Fig.3:** Solar, Radiative and Total Heat gains for the full-scale experiment during August 1<sup>st</sup> to August 5<sup>th</sup>

extraction from the conditioned space in the second test chamber. The comparative results of net space sensible cooling rate are presented in Figure 4 for the full-scale experimental measurement in both laboratories. According to Figure 4, sensible cooling rate of radiant panel can be calculated with the following equation:

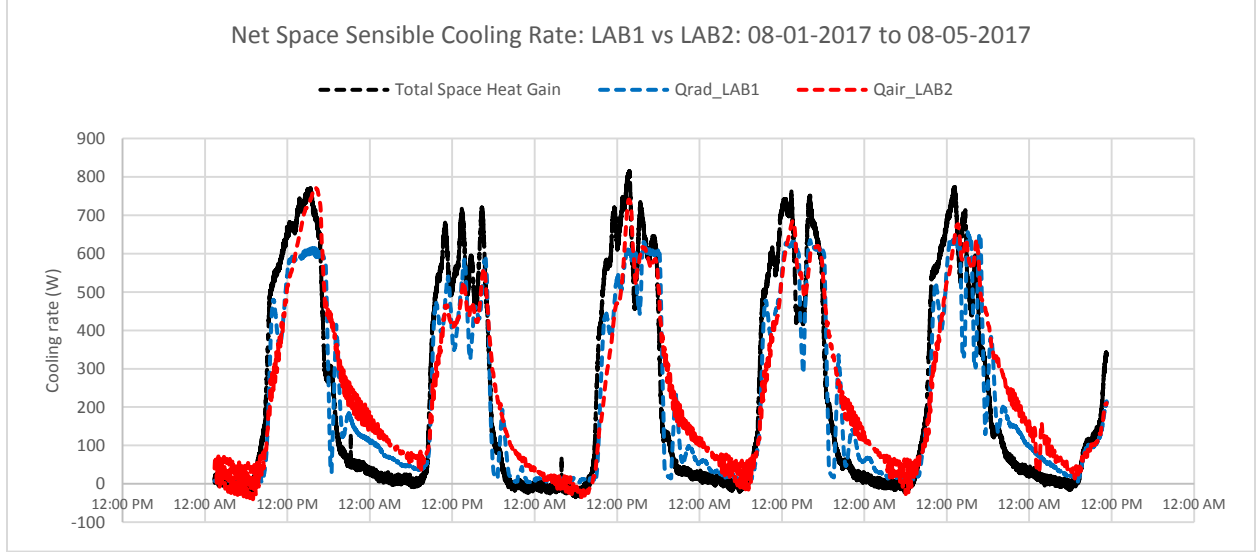


**Fig.4:** Net sensible space cooling rate for the full-scale experiment during August 1<sup>st</sup> to August 5<sup>th</sup>

$$Q_{\text{Radiant Panel}} = \dot{m}_w c_{p_w} (T_{\text{CWR}} - T_{\text{CWS}}) \quad (3)$$

where water flow rate, specific heat, chilled return water and chilled water supply to the radiant loop are denoted by  $\dot{m}_w$ ,  $c_{p_w}$ ,  $T_{\text{CWR}}$ ,  $T_{\text{CWS}}$ , respectively. For the all-air system, the net sensible cooling rate was calculated in the conditioned space as follows:

$$Q_{\text{air}} = \dot{m}_a c_{p_a} (T_{\text{RA}} - T_{\text{SA}}) \quad (4)$$

where  $\dot{m}_a$ ,  $c_{p_a}$ ,  $T_{\text{RA}}$ ,  $T_{\text{SA}}$ ,  $Q_{\text{air}}$  are air mass flow rate, specific heat of air, return air temperature, supply air temperature and cooling rate by air, respectively. As shown in Figure 4, there is a good agreement in the sensible cooling rate between radiant panel and all-air system under similar operational conditions. This shows that radiant panels can potentially be employed for providing space cooling in typical office buildings instead of an all-air system, possibly resulting in lower electricity consumption for space conditioning.

The operation of the radiant panel and all-air systems causes temperature changes in air and wall surfaces during the experiment. The wall surface temperatures were monitored with thermistors, while we measured air temperature instantaneously using six separate sensors installed on the vertical stand in the room. The results of wall surface and air temperatures are illustrated in Figure 5 throughout the five-day experiment. According to Figure 5, the use of radiant panel results in a reduction in wall surface temperature of the test chamber comparing with the all-air system. Additionally, the air temperature is essentially lower in the test chamber conditioned with radiant cooling panels. The use of radiant panel may result in stratified air temperature within the conditioned space.

The results indicates that the radiant panels can fulfill cooling needs similar to an all-air system under the same operational loads. This experiment demonstrates a comparison on the cooling performance of radiant panel versus all-air system in the identical test chambers, whose results confirm that, beside convection, radiant panels mainly extract heat from the space through direct radiative heat transfer and indirectly by cooling surrounding wall surfaces in the test chambers.

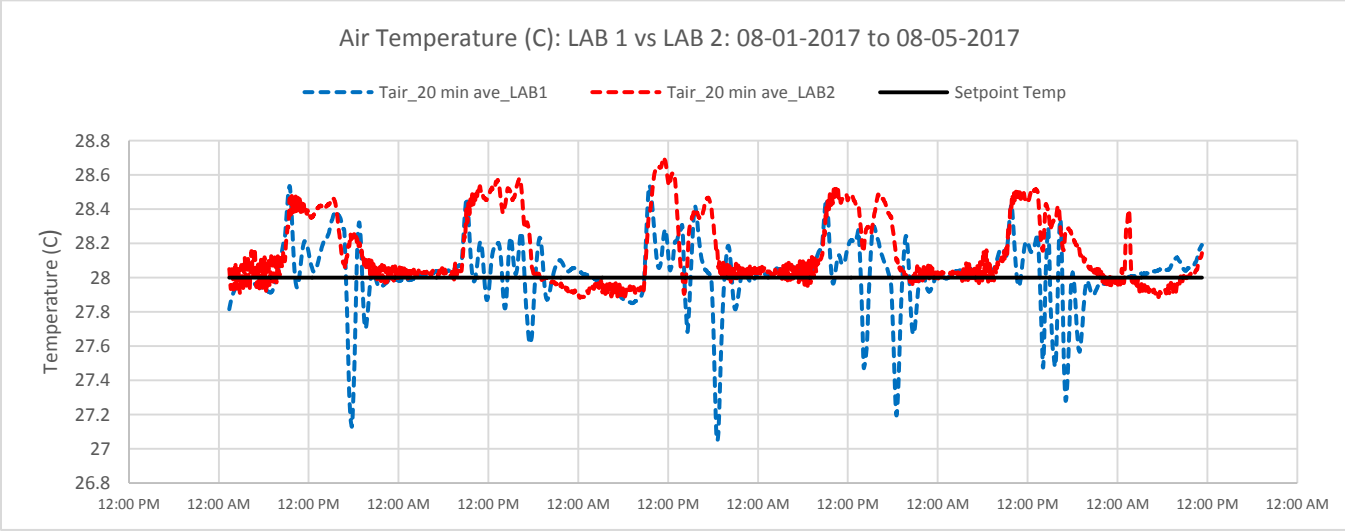
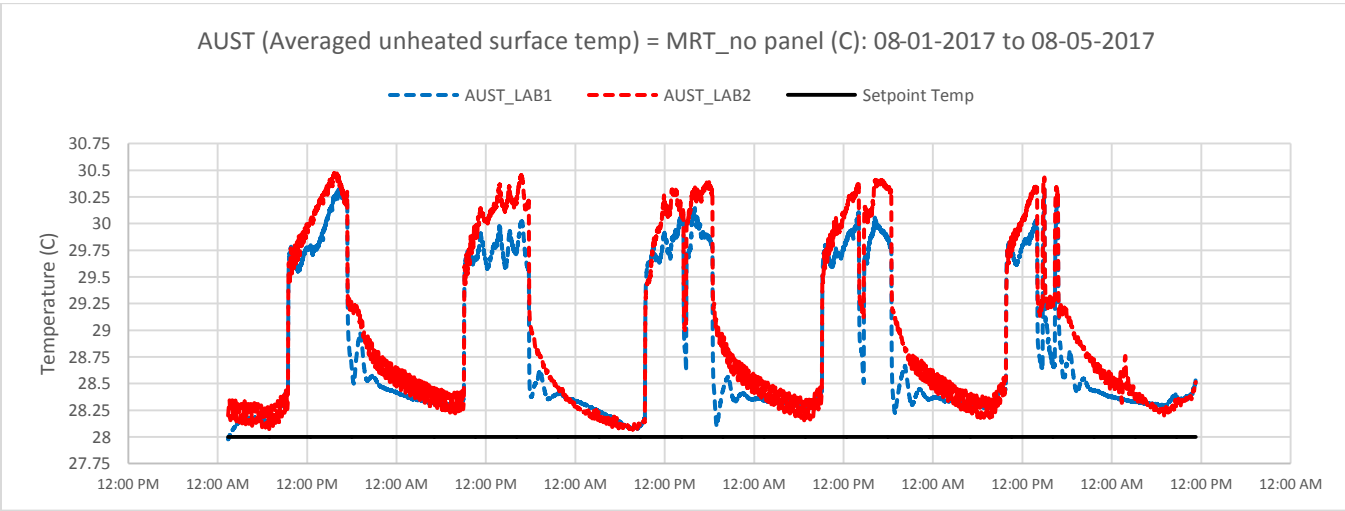
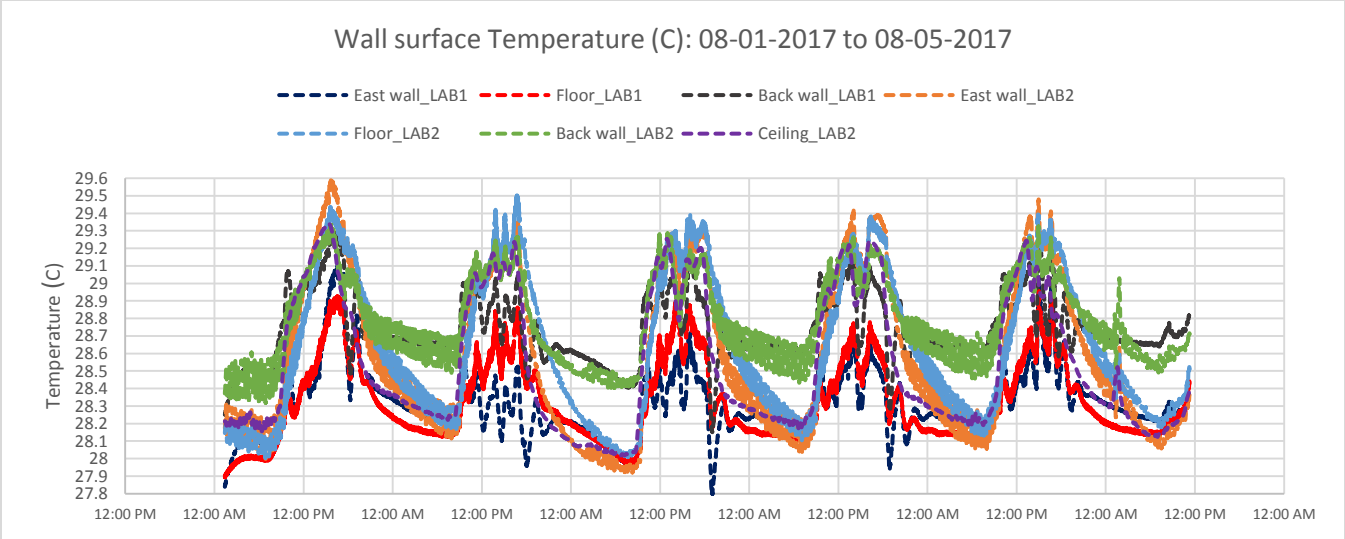


**Fig.5:** wall surface, mean radiant and air temperatures for the full-scale experiment during August 1<sup>st</sup> to August 5<sup>th</sup>

### **3-2: Experiment No. 2: Radiant panel vs All-Air system with internal loads**

The main purpose of Experiment No. 2 is to investigate the effect of internal loads on the cooling performance of radiant panel and all-air system during a six-day measurement period from August 9<sup>th</sup> to August 14<sup>th</sup> at Austin, TX. Unlike the previous experiment, we combined the radiant cooling panels with a ventilation air system in the first test chamber and examined its cooling performance with that of the second test room equipped with all-air system. Before running the experiment, one-day pre-conditioning was used to stabilize heat balance in both test chambers on August 9<sup>th</sup>.

A major portion of room heat gain is by internal sources, such as occupants, computers, etc. in the commercial buildings. The internal loads can be generally divided into convective and radiative heat gains, which are extracted either by the radiant cooling panels or all-air systems accordingly. For the present experiment, the potential cooling capacity of the combined radiant cooling panel and all-air system was examined under a combination of solar and internal convective and radiative loads. To mimic typical office space buildings, internal convective heat gains were provided by using cylinder shapes covered by thin-resistive heater element sheets to emulate convective loads resulting from occupancy, computers, etc. as shown in Figure 6. To minimize radiative energy emissions from these simulated convective loads, thin-resistive heater element sheets were covered with a low-emissivity material so they would mimic purely convective loads. The heating capacity of the resistive heater elements was precisely controlled via rheostats throughout the experiments. Additionally, the internal radiative heat gains were simulated through the use of portable high-emissivity flat resistive heater panels on the west wall of each test chamber, as illustrated in Figure 6. The resistive heater panels were powered with a variable power inverter to provide a constant internal radiative heat flux in the space. In addition, lighting equipment provided both shortwave and longwave radiation while resistive heater panels only producing longwave radiation. Thermal emissions of the resistive heater panels was controlled, and thermistors used to measure the panel surface temperature in both test chambers. In this experiment, the test chambers were subjected to solar heat gain the entire day, while the internal convective cylindrical resistive heaters were operated during working hours from 9:00 AM to 5:00 PM. The internal convective sources constantly produced 250 (W) in each test room. Moreover, the internal radiative side panel was configured for continual operation, adding 240 (W) thermal emission into the conditioned space.

Figure 7 illustrates the results of solar, internal convective and radiative heat gain in both test rooms during the six-day experiment. As shown in Figure 7, the solar radiation intensity went up to the maximum 650 (W), while internal loads were added to the space based on the aforementioned schedule. The presence of internal heaters during OFF condition (5:00 PM – 9:00 AM) represents the computers and lightings, which are normally operating and adding heat to the space even when there is no occupant in the building. In Figure 7, both radiative side panel and internal convective heaters increase the level of space heating energy according to the working schedule in a typical office environment. The results of the total heat gain, the summation of solar, electric and window conduction, are illustrated for both test rooms in Figure 7. The only difference between the total heat gain values of both test chambers was on electricity consumption by circulation fans. We employed a small fan to provide 2.8 (ACH) with average electricity consumption of 21 (W) in the first laboratory, while a larger fan was utilized to circulate ambient air with 8 (ACH) according to the ventilation standards for office spaces represented in ASHRAE 62.1. This shows the potential for radiant cooling systems to

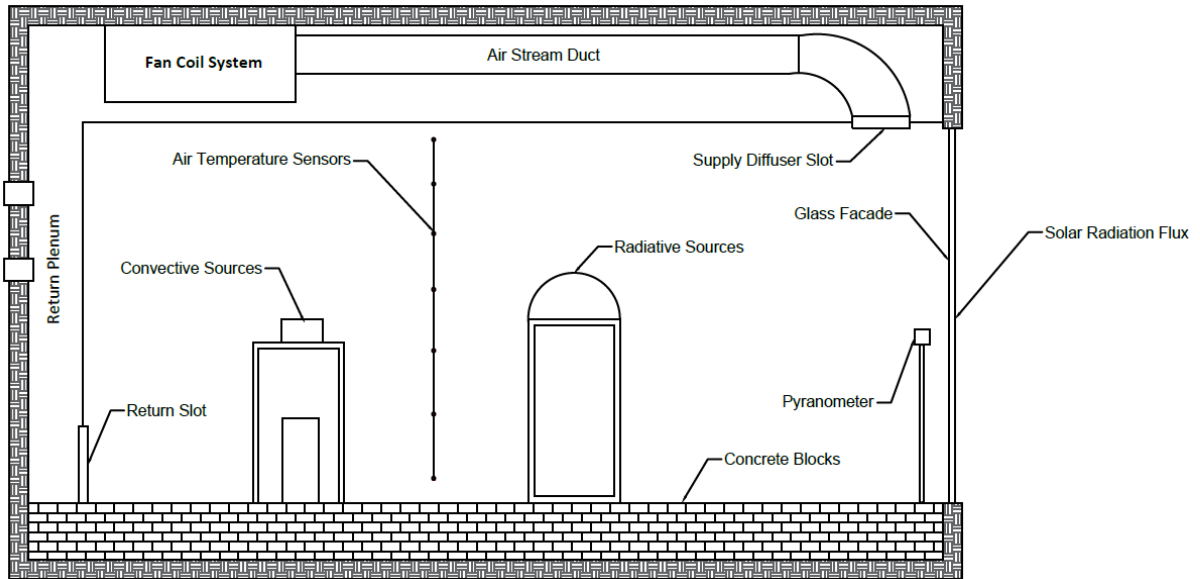


**Fig.6:** The configuration of internal radiative and convective heater sources for the full-scale experiment

reduce electricity consumption while keeping cooling performance similar to that of an all-air system under the same operational conditions.

The cooling performance of a combined radiant panel and ventilation system versus an all-air system is shown in Figure 8. This compares radiant panel and air cooling in the first test chamber with air space cooling in the second test chamber, and shows that there was good accordance between the two chambers during six-day experiment. In Figure 8, the maximum cooling capacity of the radiant panels combined with air system that provided 3 ACH was  $\sim 1200$  (W), while a minimum load of  $\sim 250$ W occurred during the night as a result of the radiative side panels in the rooms. This figure demonstrates that the radiant panel provides efficient space cooling similar to all-air system with significant lower electricity consumption.

The presence of an active cooled surface affects the heat transfer dynamics of a room conditioned with radiant panels when compared with that of an all-air system. An indication of heat transfer dynamics was demonstrated by the temperature profile of chamber surfaces. The results for wall surface temperature are shown in Figure 9. According to Figure 9, wall surface temperatures were generally lower for the laboratory conditioned with radiant cooling panel comparing with those of the all-air system because radiant panel extracted heat from the envelope through radiative heat transfer. In Figure 9, mean radiant temperature for wall surfaces (AUST) in lab 1 was higher than that of the second test chamber. This figure also addressed MRT was almost 2 degrees greater than zone air set point temperature (28 C) during the operation of full-scale experiment. Additionally, the air temperature measured by thermistors installed in the vertical stand represented the air temperature profile in the vertical direction from the floor to the ceiling. As shown in Figure 9, the air temperature was higher in the test chamber conditioned with all-air system comparing with the room equipped with radiant cooling panels.

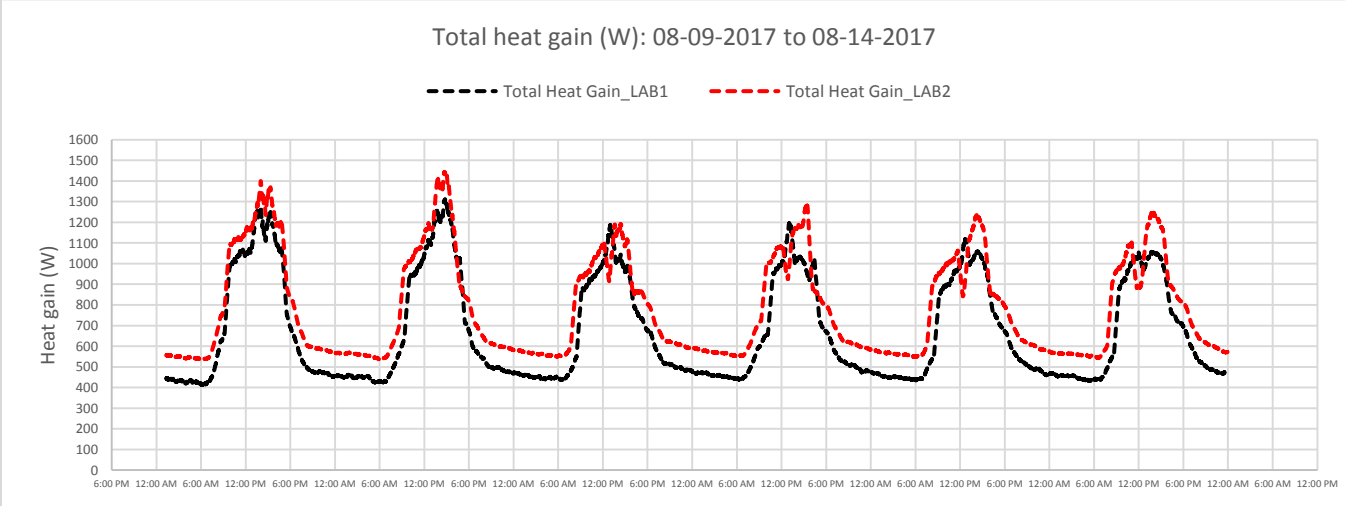
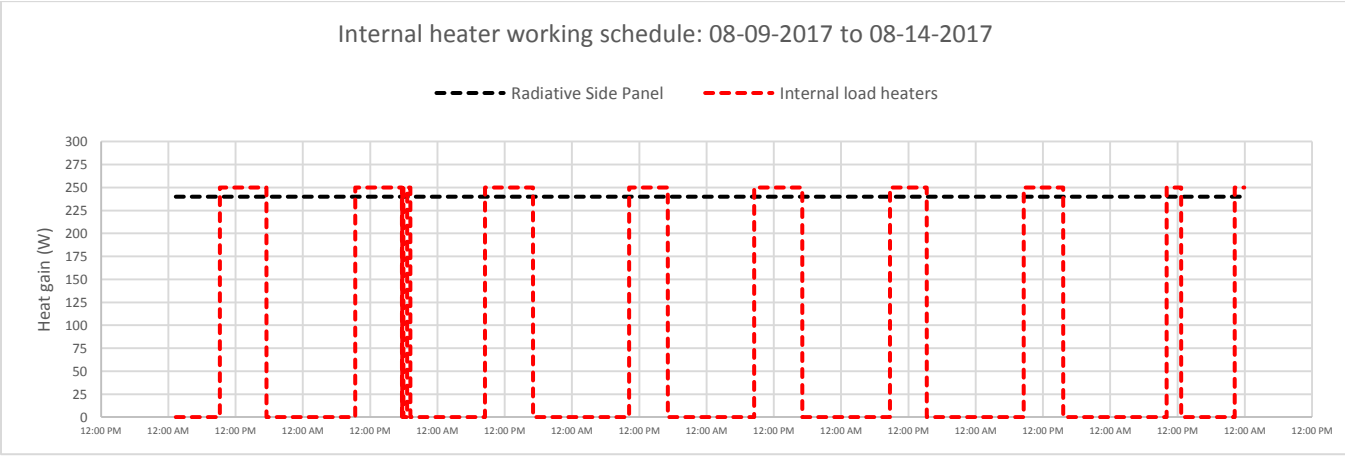
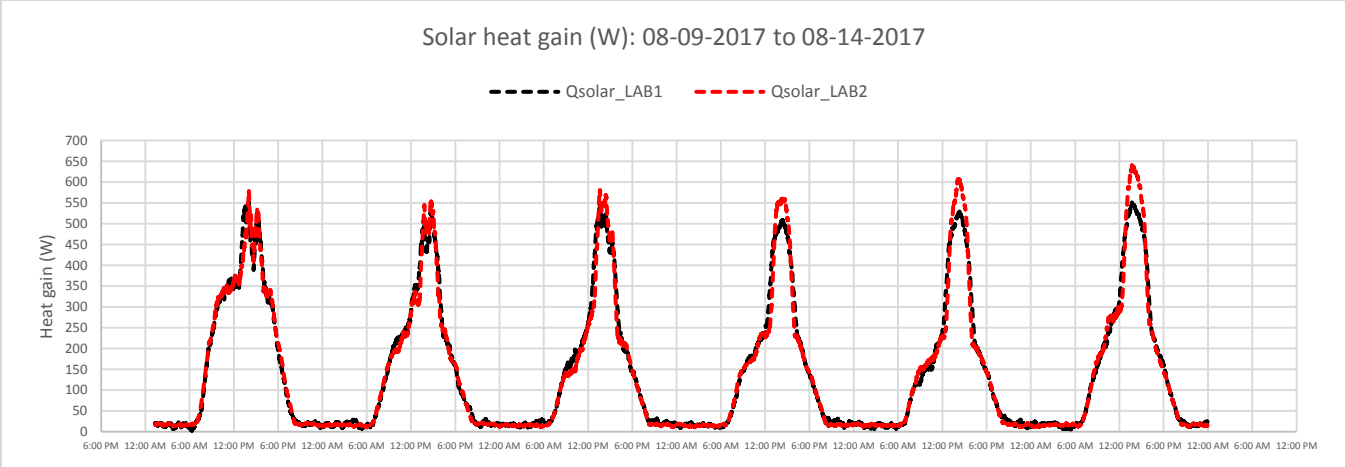


**Fig.7:** Solar, internal convective, radiative heat gains for the full-scale experiment during August 9<sup>th</sup> to August 14<sup>th</sup>

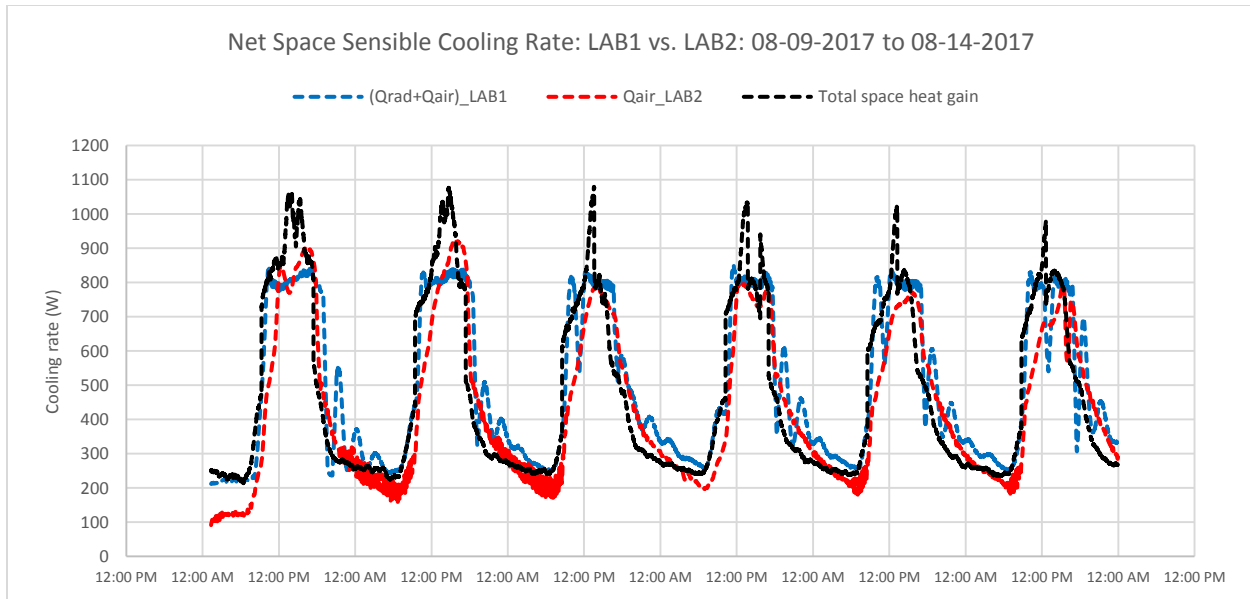


**Fig.8:** Net space cooling rate for the full-scale experiment during August 9<sup>th</sup> to August 14<sup>th</sup>

The present experiment represents the effects of internal loads. The experiment shows a combined radiant panel with a ventilation system can maintain heat extraction rates similar to an all-air system. The presence of radiant cooling panel in the room results in significant heat extraction from the space directly through radiative heat transfer and indirectly by cooling surrounding surfaces, causing efficient temperature reduction in wall surfaces during daily operation due to decreasing heat accumulation in the envelope. Another consequence of radiant cooled ceiling is to stabilize temperature stratification in the space conditioned with radiant panel while achieving thermal comfort in the office space. On the other hand, an all-air system preserves space cooling majorly through convective heat transfer. The operation of all-air system will increase heat extraction speed in the room via cooled air circulation as a result of increase in convection rate on interior wall surfaces. However, Averaged Unheated Surface Temperature (AUST) is relatively lower for the room conditioned with radiant panels comparing with that of all-air systems.

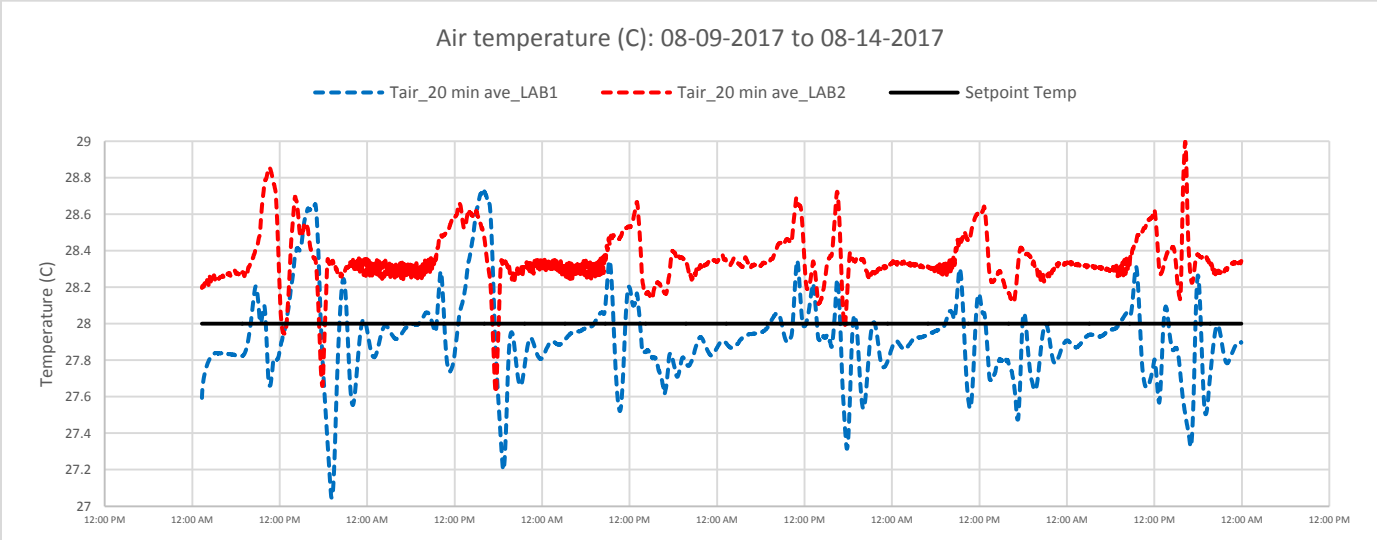
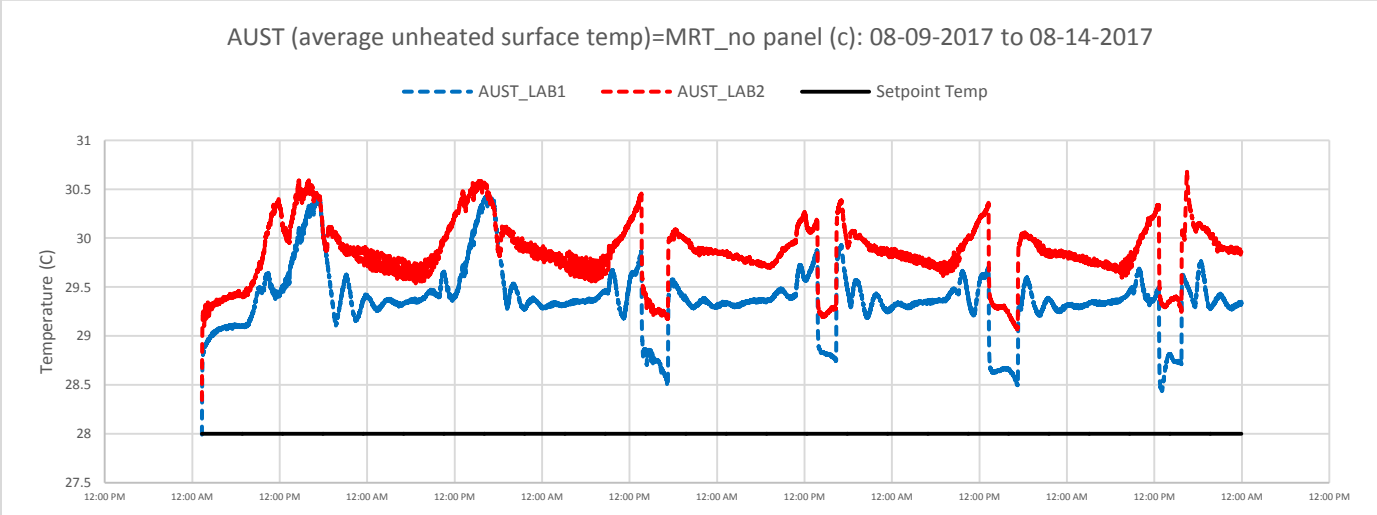
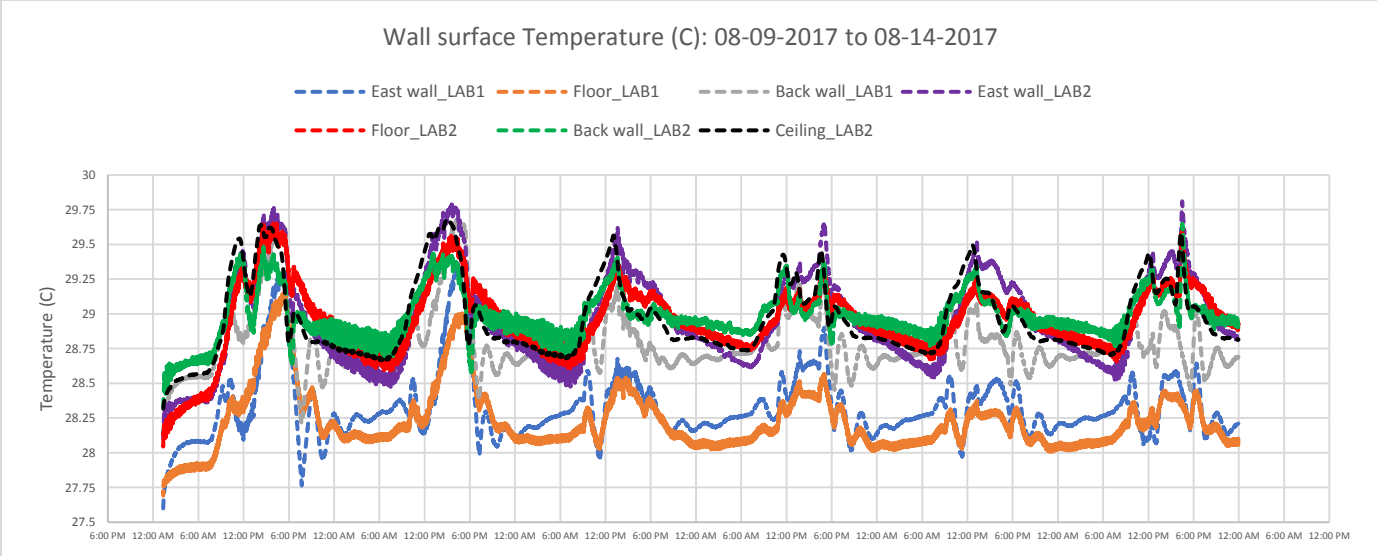


**Fig.9:** Wall surface, air temperature profiles for the full-scale experiment during August 9<sup>th</sup> to August 14<sup>th</sup>

### **3-3: Experiment No. 3: Radiant panel vs All-Air system with constant internal loads**

The main purpose of Experiment No. 3 is to investigate the effects constant internal heaters on the cooling performance of radiant panel and all-air system during three-day full-scale experiment from August 17<sup>th</sup> to August 20<sup>th</sup> in Austin, TX. In this experiment, we examined the cooling performance of radiant panel versus all-air system under constant 250 (W) internal convective and radiative loads. A one-day pre-conditioning period was run prior to the full-scale measurements to stabilize heat balance in the test rooms.

This experiment investigated the impact of internal cylinder and box heaters on the heat balance of the test chambers. The internal cylinder and box heaters to simulate occupancy were located in the middle of the room to secure uniform heat emission to all interior wall surfaces. The objective of utilizing internal cylinder and box heaters was to emulate occupancy and computers in typical office spaces. The internal cylinder and box heaters were composed of thin-resistive heater element sheets, which were also covered with low emissivity coverings to minimize radiative energy emissions. The thermal emissions of the internal heaters was controlled using rheostats, and their surface temperatures were measured by thermistors installed on the element sheets. Throughout the experiment the internal cylinder and box heaters were constantly adding 250(W) day and night to the space. Therefore, either the mixed radiant panel and ventilation system or all-air system was responsible for extracting the solar and internal loads from the test rooms. Figure 10 displays the solar heat gain, internal load working schedule and total heat gains in both test chambers during the experiment. The average solar heat gain was 700 (W), causing to increase the level of thermal energy in the room required to be removed by the cooling systems.

The net space sensible cooling rate are presented for the radiant panel and all-air system in Figure 11. According to Figure 11, both combined radiant panel with ventilation system and all-air system managed to handle all loads in the test chambers. In this experiment, the radiant panel was operated at its maximum cooling capacity of 850 (W), while the rest of heat was extracted by cooled circulating air in the room. In the second test chamber, all-air system was responsible to remove the maximum cooling load of 1200 (W) during the experiment. The results of temperature profiles for wall surfaces and ambient air are illustrated for the experiment in Figure 12. As shown in Figure 12, the wall surface temperatures were generally lower for the room conditioned with combined radiant panel with ventilation system when compared with the all-air system. Comparing the MRT, averaged unheated surface temperature was relatively higher for the walls of the second test room conditioned with all-air system, while average measured air temperature was lower in the first test chamber with radiant panel.

This experiment shows that radiant panels can manage cooling demand in a room with internal heat sources in combination when used in combination with a small fan system for ventilation with similar cooling performance comparing to the all-air system. The result is a reduction in electricity consumption in the radiant panel configuration compared with that of the all-air system. The use of radiant panels results in significant temperature decrease in both envelope and ambient air due to an efficient-direct radiative heat transfer and indirect cooling of the surrounding wall surfaces.

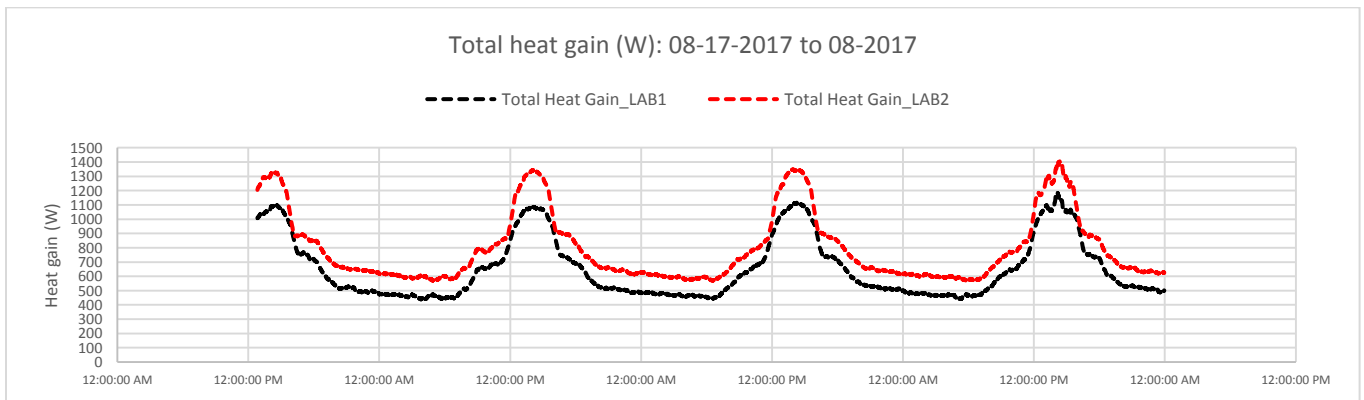
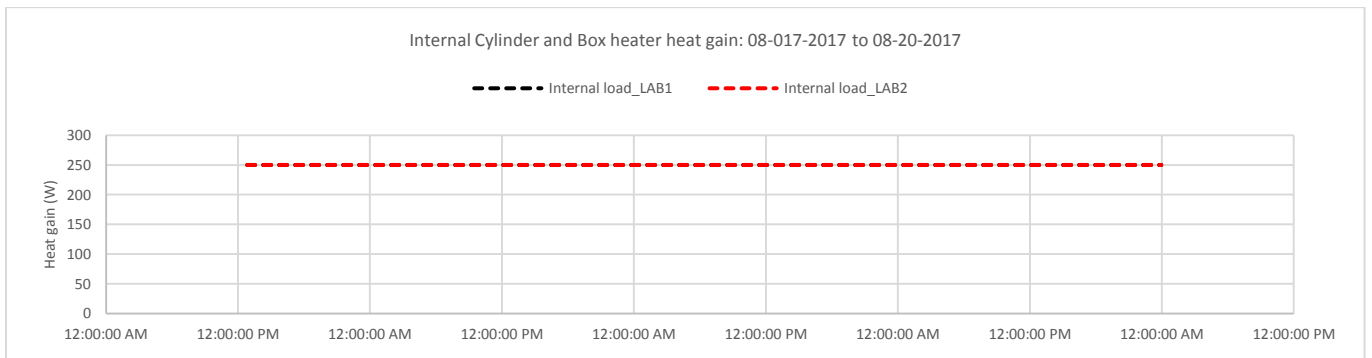
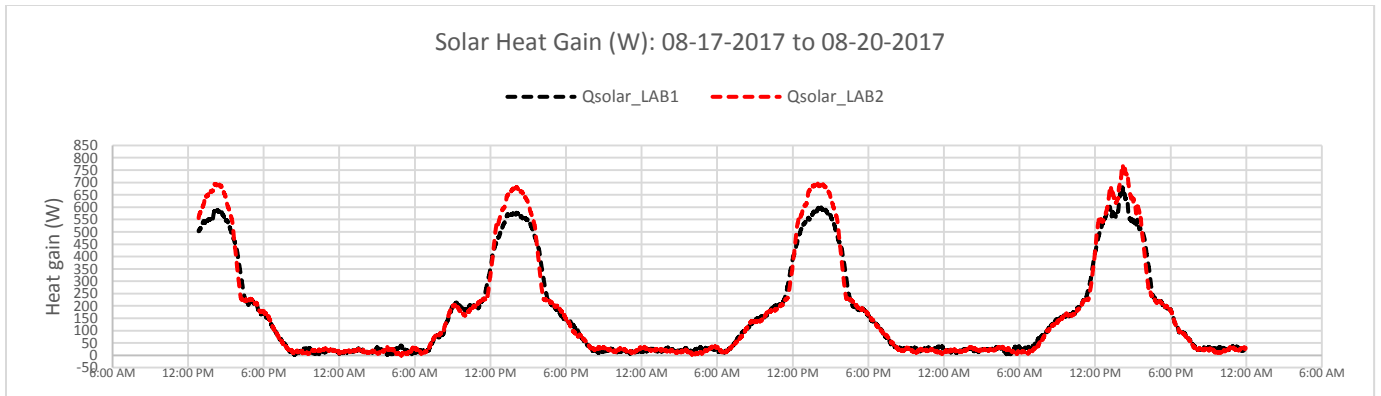


**Fig.10:** Solar, internal convective, radiative heat gains for full-scale experiment during August 17<sup>th</sup> to August 20<sup>th</sup>

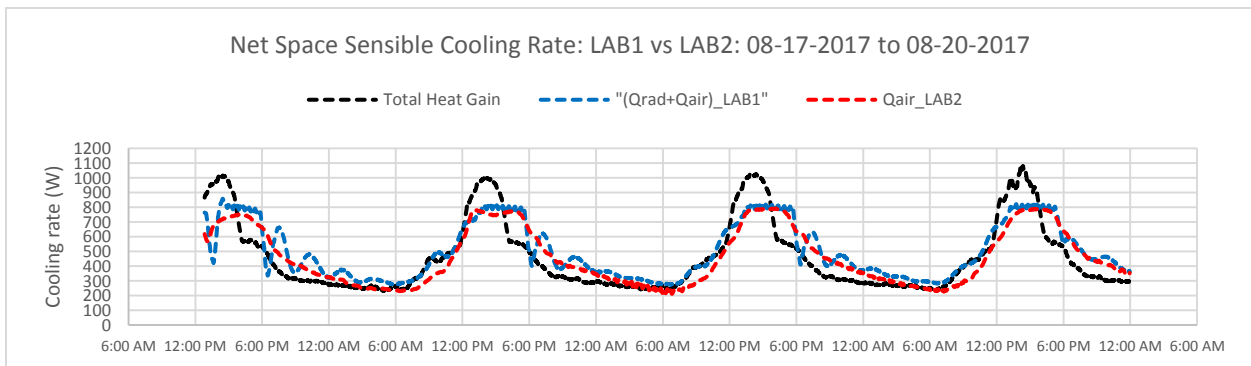


**Fig.11:** Net space sensible cooling rate for full-scale experiment during August 17<sup>th</sup> to August 20<sup>th</sup>

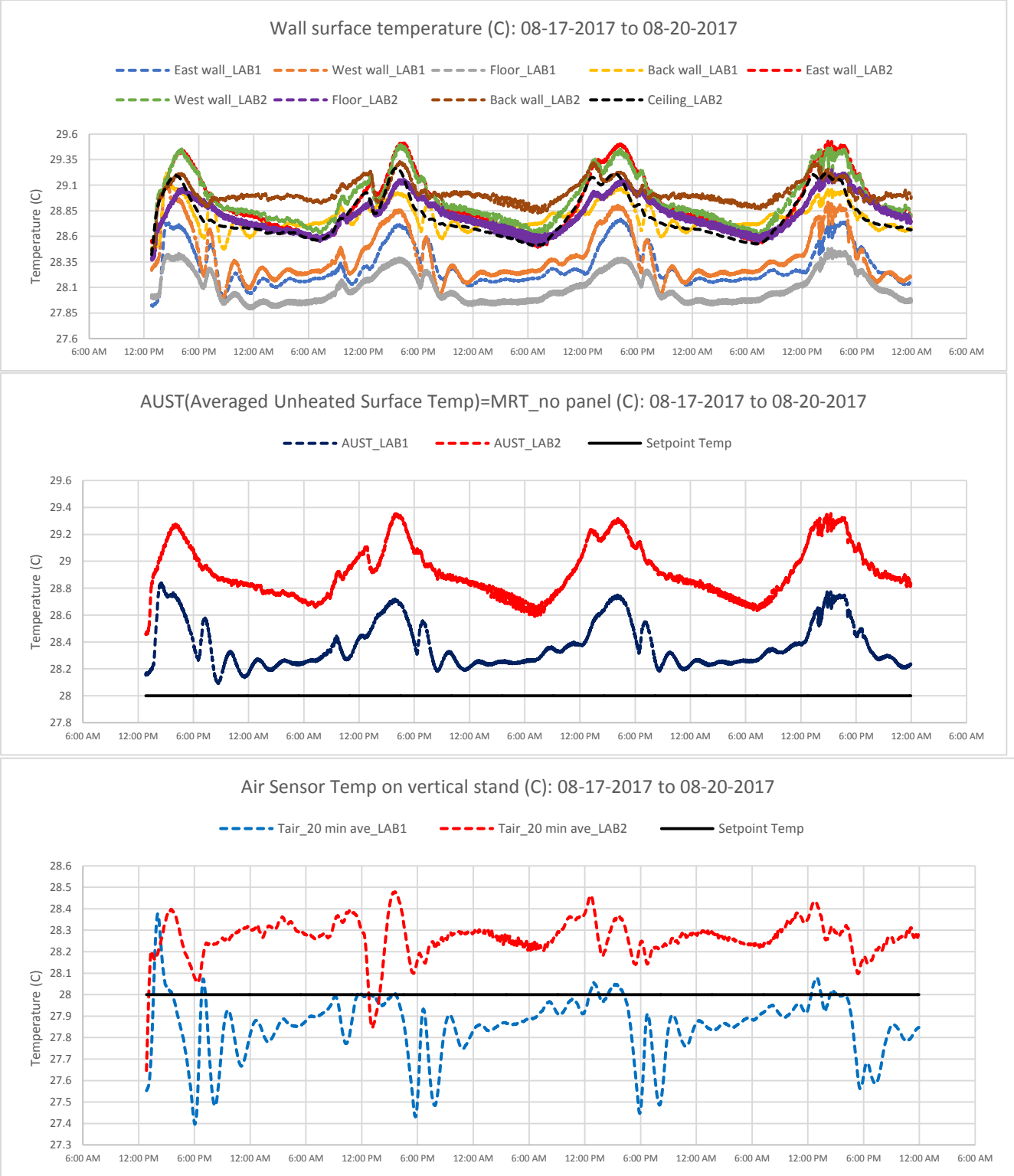


**Fig.12:** wall surface, MRT, Air temperatures for full-scale experiment during August 17<sup>th</sup> to August 20<sup>th</sup>

### **3-4: Experiment No. 4: Radiant panel vs All-Air system with internal loads in typical office working schedule**

The main purpose of this experiment is to investigate the cooling performance of the radiant panel and all-air systems in a test chamber subjected to internal heaters using a working schedule appropriate for a typical office space. The period of the experimental measurement was from August 22<sup>nd</sup> to August 24<sup>th</sup> in Thermal Façade Laboratory in University of Texas at Austin. Before running the experiment, a one-day pre-conditioning period was used to stabilize heat balance in the test rooms.

The present experiment was designed to mimic the effects of internal loads in a normal work operating schedule for a typical office space. In this experiment, internal cylinder and box heaters were employed to constantly add 250 (W) during the office working hours. The test chambers were subjected to normal solar radiation as well as internal convective and radiative loads from 7:00AM to 5:00 PM throughout the experiment. During this time, a combined radiant panel with ventilation system was working in the first test chamber, while an all-air system was used to remove space heat in the second test chamber. From 5:00 PM to 7:00 AM, the HVAC systems, consisting of cooling coil, fans, pumps, etc., were turning off in both test chambers. The major reason for this was to emulate normal HVAC operation schedule in commercial buildings. During the so-called OFF condition (5:00 PM-7:00 AM), the test chambers were experiencing a free-floating condition where the air temperature increased in the occupied zone. As the HVAC system were restored during the so-called ON period, both radiant panel and all-air system worked to remove the thermal energy stored during the free-float period and restore the set point temperature.

The cooling equipment was designed to remove solar and internal heat gains from the test rooms. The results of solar heat gain, working schedule for internal convective and radiative heaters and total heat gain are illustrated in Figure 13. Solar heat gain varied throughout two days with the average value of 700 (W). The results of total heat gain as the sum of electric load, solar heat gain and conduction through façade, are also displayed for the experiment. The main difference between total heat gain was the electricity consumption by circulating fans in the test rooms. In Figure 14, we have compared the cooling performance of the two test chambers by using net space sensible cooling rate as the metric, where the sum of heat extraction rate by radiant panel and air circulation system in the first laboratory was compared with heat removal by the fan coil in the second test room. According to Figure 14, there was a good accordance between the cooling capacity of combined radiant panel with ventilation system versus the all-air system. As shown, the sensible cooling rate went to zero during OFF condition for both sets of cooling equipment. However, as soon as the HVAC systems were restored at 7:00 AM, both radiant panel and all-air system facilitated heat extraction with full-cooling capacity according to the controller command until the set point for the space was restored..

The cooling performance of the radiant panel and all-air system results in a considerable change in the temperature profile for the air and envelope, which are shown in Figure 15. In this Figure, wall surface temperatures were generally lower for the test room conditioned with radiant panel comparing with those of the all-air system. Also, the averaged unheated surface temperature or MRT was significantly lower for the test room with radiant panel due to efficient heat extraction by radiative heat transfer comparing to that of the all-air system in the second laboratory. According to Figure 15, the measured air temperature

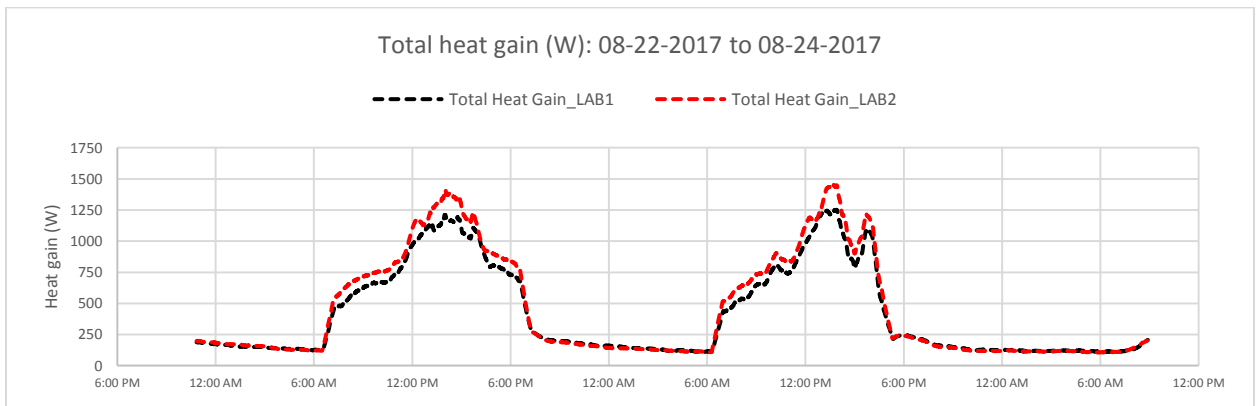
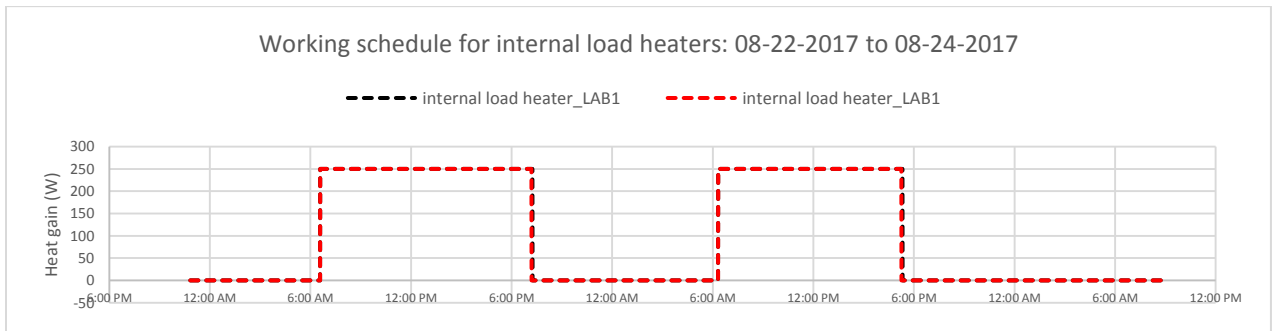
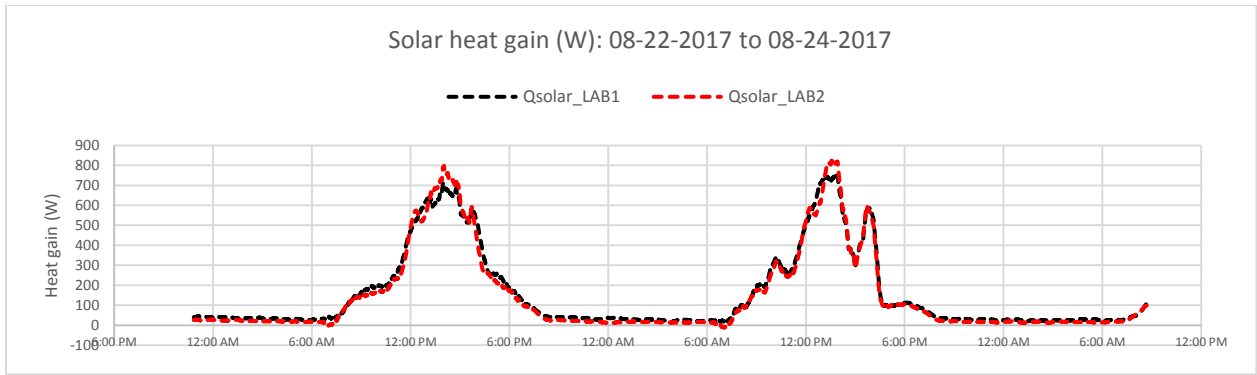


**Fig.13:** Solar, internal convective, radiative heat gains for full-scale experiment during August 22<sup>nd</sup> to August 24<sup>th</sup>

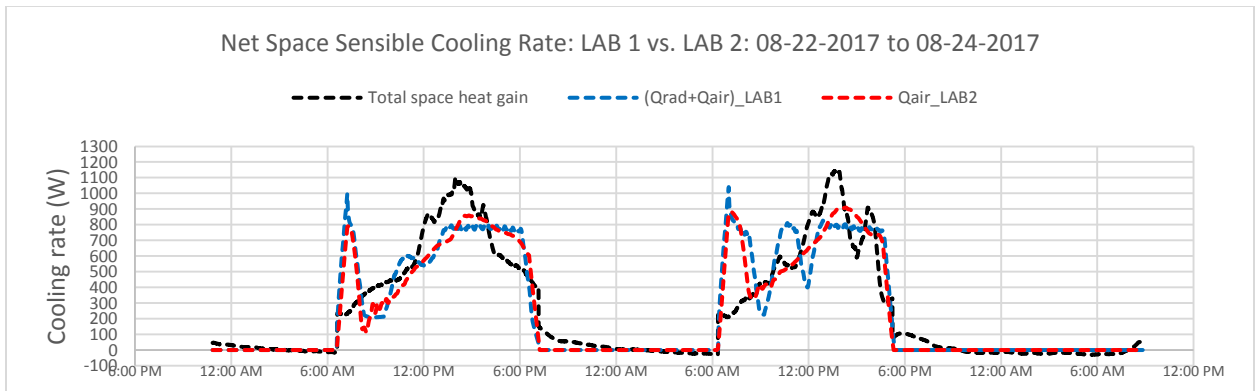


**Fig.14:** Net space sensible cooling rate for full-scale experiment during August 22<sup>nd</sup> to August 24<sup>th</sup>

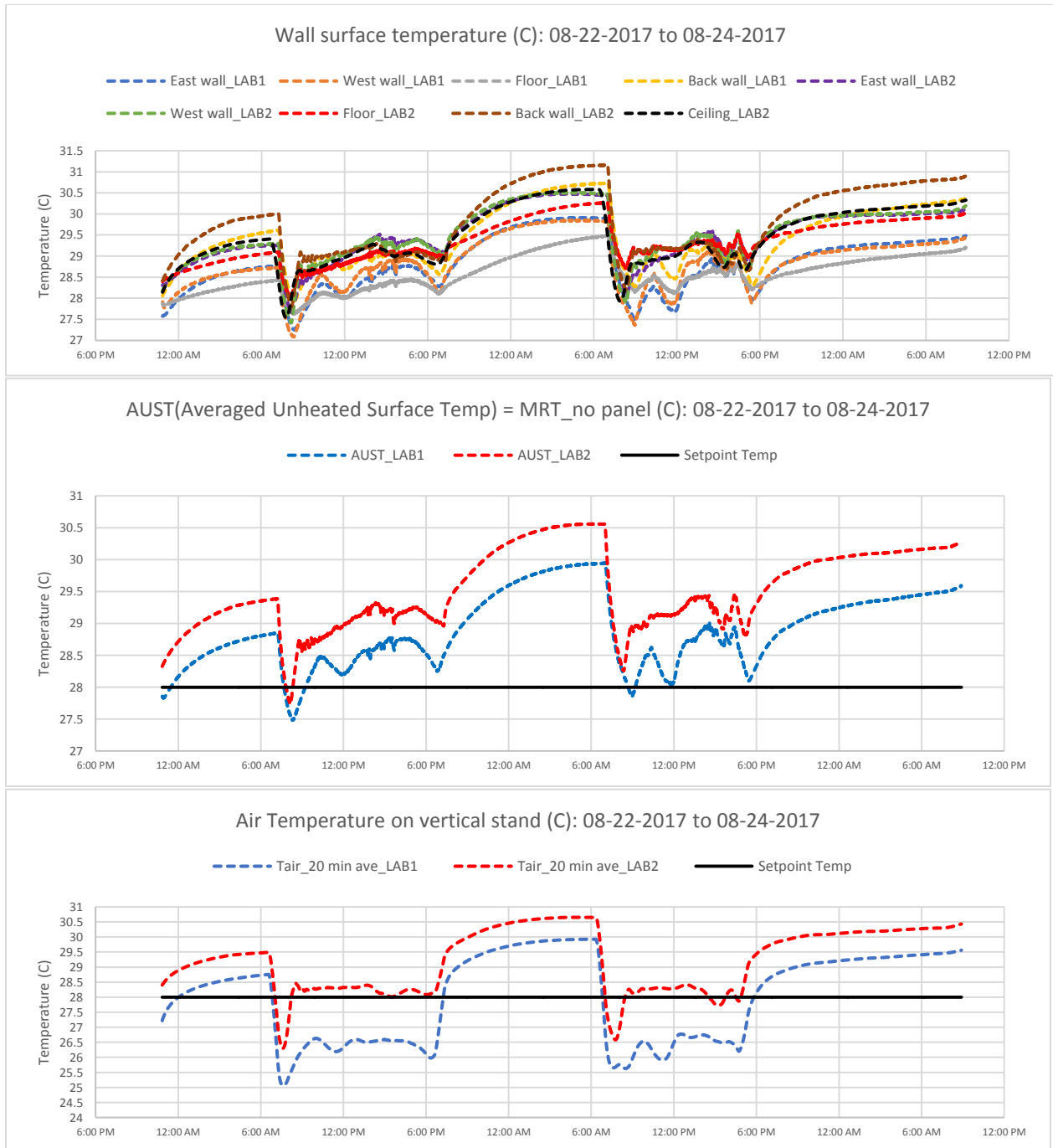


**Fig.15:** wall surface, MRT, Air temperatures for full-scale experiment during August 22<sup>nd</sup> to August 24<sup>th</sup> changed during ON and OFF conditions, while air temperature was relatively higher for all-air system in the second test chamber comparing with radiant panel.

These results show that the radiant panel system was capable of maintaining comfort in the space during ON-OFF schedule used in typical office buildings as well as the all-air system. The use of combined radiant panel and ventilation system facilitated heat extraction from the envelope on the daily operation of typical office spaces.

### **3-5: Experiment No. 5: Radiant panel vs All-air system cooling performance under dominant solar load**

The main objective of this experiment was to investigate the cooling performance of a radiant panel versus an all-air system under dominant solar load from August 31<sup>st</sup> to September 3<sup>rd</sup> in Thermal Façade Laboratory in University of Texas at Austin. As before, there was a one-day pre-conditioning performed to allow both the radiant cooling panel and all-air systems to stabilize heat balance before running the full-scale experiment.

The present experiment was designed to determine the effects of pure solar load on the cooling performance of a radiant panel and all-air system according to the working schedule of commercial buildings. Note that the first test room was equipped with combined radiant panel with 2.8 (ACH) ventilation system, while an all-air system was used in the second laboratory, capable of providing 8 (ACH) for the ventilation requirement as addressed by ASHRAE 62.1 in office spaces. The test chambers were subjected to dominant solar heat gain entering from the south-facing glass façade without any internal load. The result of solar heat gain is displayed in Figure 16 for the full-scale experiment. Although the weather was partly cloudy, the maximum solar heat gain was 1000 (W). The total heat gain in both test chambers is shown in Figure 16 during the three-day experiment as the summation of solar heat gain, electric load and conduction through the façade. According to Figure 16, the total heat gains of the test chambers were different because of their using distinct fan configurations with different electricity consumptions. The test rooms were operating according to ON-OFF schedule in typical office buildings. The cooling equipment started to work from 7:00 AM to 6:00 PM non-stop (ON condition), and turned off from 6:00 PM to 7:00 AM (OFF condition). To analyze cooling capacity, net space sensible cooling rate was used as the metric to check cooling performance of the radiant panels versus that of the all-air system. Figure 17 shows that the cooling capacity of radiant panel was equal to zero during the OFF condition, suddenly ramps upward as the cooling system is restored, and then modulates the sensible cooling rate for the rest of the day. The same happened for the all-air system. As can be seen in Figure 17, the all-air system was capable of meeting the cooling demand during peak heat gain just as well as the combined radiant panel and ventilation system.

The cooling performance of the radiant panel and all-air system affects the temperature profile in the air and wall surfaces in the test chambers. The results of wall surface temperature are represented in Figure 18, where it can be seen the surface temperatures were generally higher in the test room conditioned with all-air system compared with those of the combined radiant panel and ventilation system. The averaged unheated surface temperature of walls was almost 0.5 (C) higher than the zone air set point temperature in the room conditioned with radiant panels, while it was 1.5 (C) higher than the set point temperature for the all-air system. This shows that the radiant panels can efficiently extract heat from the space. The air temperature measured by six separate temperature sensors on the vertical stand, was also lower in the test room conditioned with radiant panels when compared with the all-air system. Additionally, it should be noted that the free-float temperature increased to the range of 29.5-31.5 (C) in the test chambers when the systems were off.

From the results, the cooling performance of the radiant panel and all-air systems was dependent on the solar load during cooling operations in typical office spaces. For radiant panels, a major portion of solar load was directly removed through shortwave radiation while the rest of the heat was absorbed in the envelope and then extracted either by longwave radiation or convection in the space. However, the all-air system was capable of removing space heat through convective heat transfer by circulating chilled

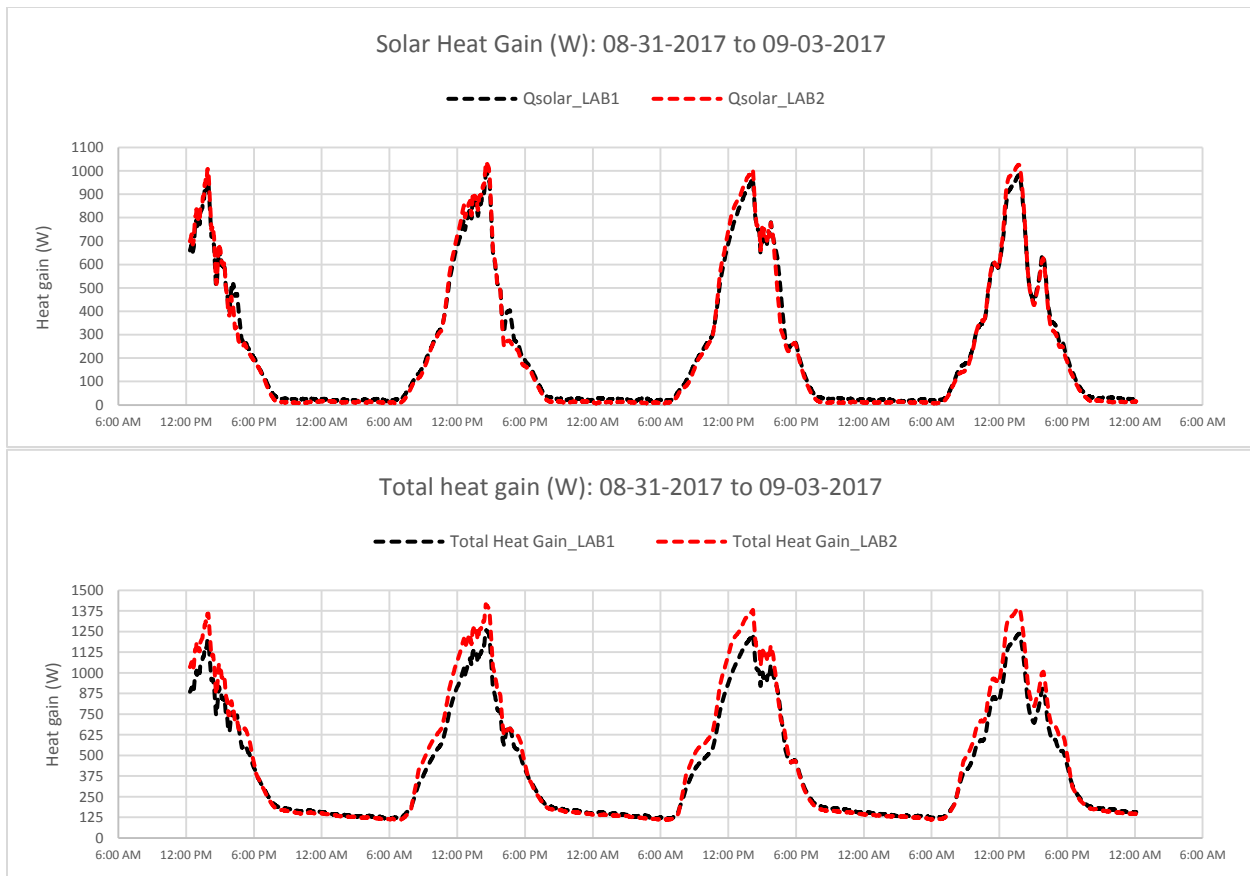


**Fig.16:** Solar and total heat gain for full-scale experiment during August 22<sup>nd</sup> to August 24<sup>th</sup>

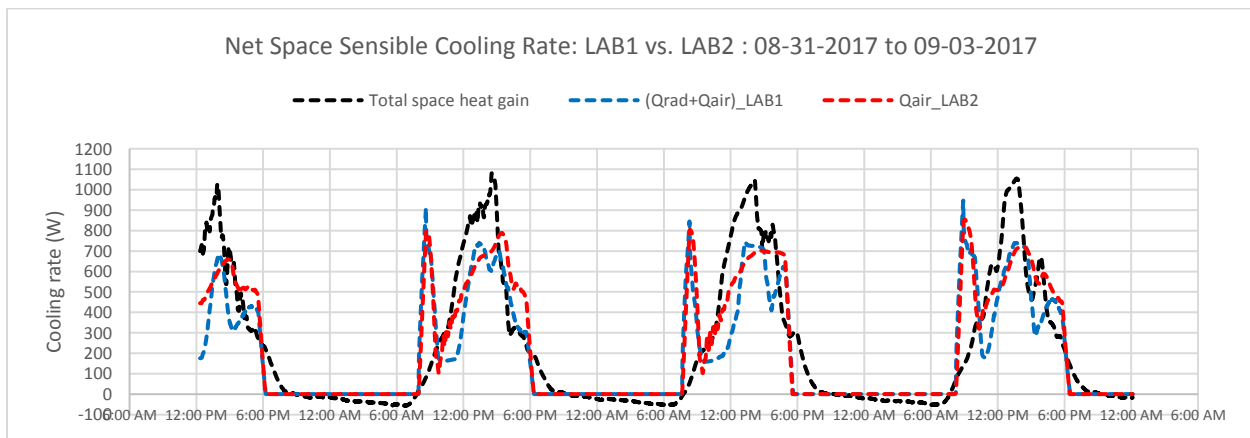


**Fig.17:** Net space sensible cooling rate for full-scale experiment during August 31<sup>st</sup> to September 3<sup>rd</sup>

air. The present experiment indicates the the choice of either radiant panel or all-air system can provide space cooling; however, the use of combined radiant panel with a reduced-size ventilation system will save electrical energy in the commercial building scale comparing with the all-air system.

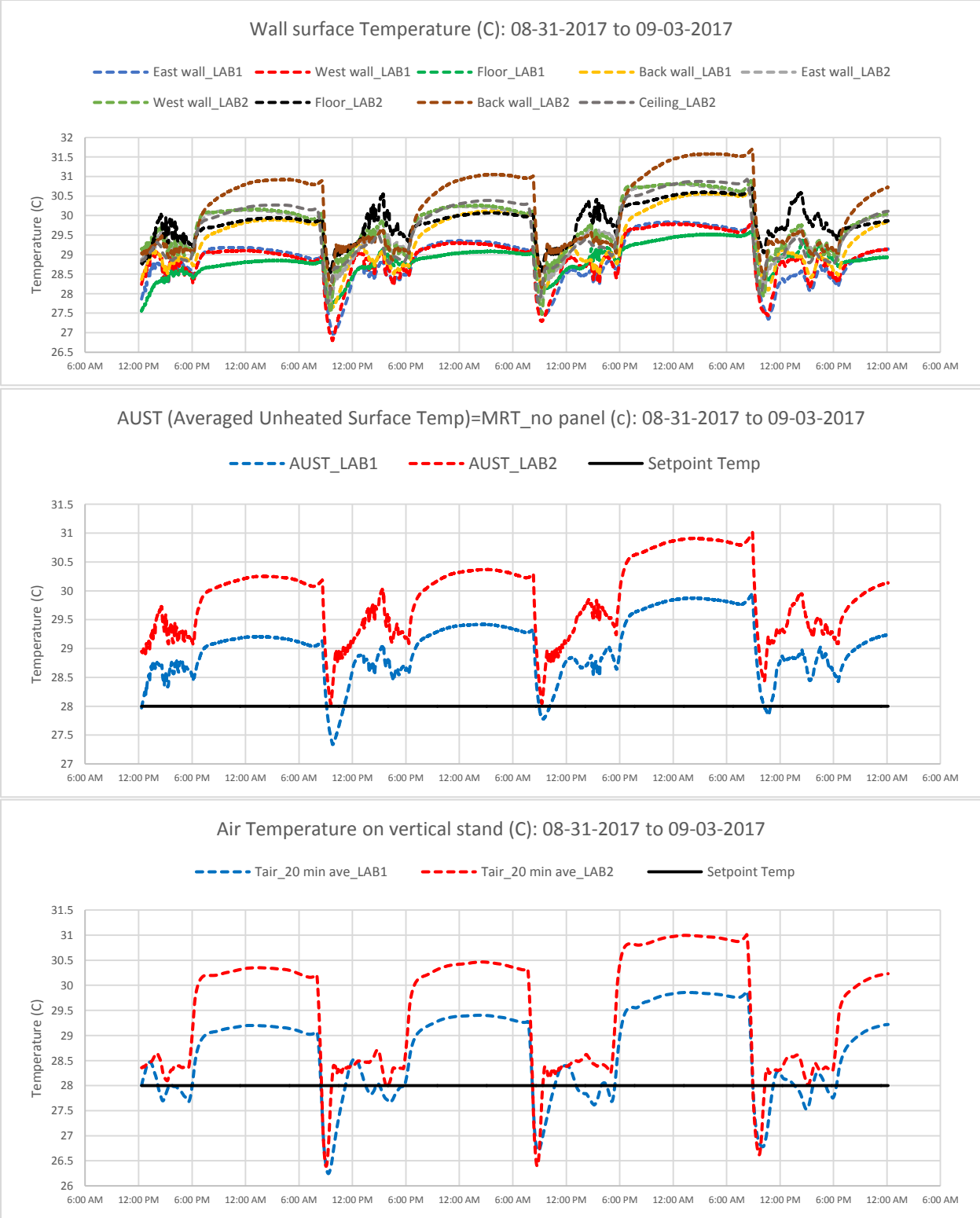


**Fig.18:** wall surface, MRT, Air temperatures for full-scale experiment during August 31<sup>st</sup> to September 3<sup>rd</sup>

---

## REFERENCES

---

- [1] Causone F, Corgnati SP, Filippi M, Olesen BW. 2009. "Experimental evaluation of heat transfer coefficients between radiant ceiling and room". *Energy and Buildings*;41 (6):622–8.
- [2] Miller, P. L. and Nash, R. T. 1971. "A further analysis of room air distribution performance." *ASHRAE Transactions* 77(2):205
- [3] Miller, P. L. and Nevins, R. G. 1969. "Room air distribution with an air distributing ceiling – Part II." *ASHRAE Transactions* 75:118
- [4] Miller, P. L. and Nevins, R. G. 1970. "Room air distribution performance of ventilating ceilings and cone-type circular ceiling diffusers." *ASHRAE Transactions* 7660:186
- [5] Miller, P. L. and Nevins, R. G. 1972. "An analysis of the performance of room air distribution systems." *ASHRAE Transactions*.
- [6] Novoselac, Clark, Goldstein, Peeters. "Development of Internal Surface Convection Correlations for Energy and Load Calculation Methods- ASHRAE Research Project 1416-RP Final Report. ASHRAE 2012
- [7] Peeters L. and Novoselac A., "Impact Of Human Activity On Unsteadiness Of Airflow And Convective Heat Transfer In Indoor Environmental Studies". *Proceeding of Indoor Air 2011*, Indoor Air 2011, June 5-10, Austin, TX.
- [8] Fredriksson J, Sandberg M, Moshfegh B. "Experimental investigation of the velocity field and airflow pattern generated by cooling ceiling beams". *Building and Environment* 36 (2001) pp. 891-899.
- [9] J. Feng, S. Schiavon, F. Bauman, "Cooling load differences between radiant and air systems", *Energy and Buildings*, Volume 65, Pages 310-321.
- [10] J. Feng, F. Bauman, S. Schiavon, "Experimental comparison of zone cooling load between radiant and air systems", *Energy and Buildings*, Volume 84, Pages 152-159.